AIAA JOURNAL
Vol. 32, No. 12, December 1994

Coupled FEM-BEM Approach for Mean Flow Effects on Vibro-Acoustic Behavior of Planar Structures

Franck Sgard,* Noureddine Atalla,† and Jean Nicolas‡
University of Sherbrooke, Sherbrooke, Quebec J1K 2R1, Canada

The originality of the present paper lies in the development of a formulation accounting for mean flow effects on the forced vibro-acoustic response of a baffled plate. The importance of these effects on the vibrational behavior of the plate, as well as on its acoustic radiation pattern, is investigated for a baffled plate with different kinds of boundary conditions. The analysis is based on a finite element method for the calculation of the plate transverse vibrations and the use of the extended Kirchhoff's integral equation to account for fluid loading with mean flow. A variational boundary element method is used to compute the acoustic radiation impedance. The formulation shows explicitly the effects of mean flow in terms of added mass, stiffness, and radiation damping. Details of the formulation as well as its numerical implementation are expounded, and results showing the effect of mean flow in light and heavy fluid on the vibro-acoustic quantities, such as mean square velocity and radiated acoustic power, are presented. It is seen that the effects of a mean flow amount to a decrease of the natural frequencies of the plate, a small damping effect on the vibrations, and a change in the radiated acoustic power when compared with the no-flow case. Besides, these effects increase with the flow speed. The negative stiffness added by the flow is shown to be mainly responsible for the natural frequency shift effect. The changes in the radiated acoustic power are explained in terms of important changes in the radiation efficiencies and modal cross-coupling induced by the flow.

Nomenclature

a	= plate length
$[B_{\text{coup}}]$	= reduced coupling impedance matrix, $[Z_{\text{coup}}] = [S]^T[B_{\text{coup}}][S]$
$[B_{\text{ray}}]$	= reduced radiation impedance matrix, $[Z_{\text{ray}}] = [S]^T[B_{\text{ray}}][S]$
b	= plate width
c_0	= sound speed
$dS(M)$, $dS(Q)$	= surface elements surrounding points M and Q on the plate
E	= Young's modulus
$\{F_{\text{ac}}\}$	= acoustical force nodal vector
$\{F_{\text{mech}}\}$	= mechanical force nodal vector
$F(\boldsymbol{w}, p_{\text{ac}})$	= structural energy functional
f	= mechanical force acting on the plate
$G(M, Q)$	= modified Green's function
h	= plate thickness
$[K_s]$	= structural stiffness matrix
$[\tilde{K}_s]$	= structural stiffness matrix accounting for structural damping
k_0	= acoustic wave number, Ω/c_0
M, Q	= points on the plate
$[M_s]$	= structural mass matrix
M_V	= point in space
M_∞	= Mach number, U_∞/c_0
$\{N^{w_n}\}$	= shape function vector for normal displacement w_n
p_{ac}	= acoustic pressure
$Re[\cdot]$	= real part of $[\cdot]$
$[S]$	= transformation matrix defined by $\{w_{n_i}\} = [S]\{W_i\}$
S_p	= plate area
$T(\boldsymbol{w}, \boldsymbol{w})$	= kinetic energy of the structure
U_∞	= flow speed
u_x	= x component of the particle acoustic velocity
u_z	= z component of the particle acoustic velocity
$\langle V^2 \rangle$	= plate mean square velocity
$V(\boldsymbol{w}, \vec{\boldsymbol{w}})$	= strain energy of the structure
W_{ac}	= work done by the acoustic forces on the structure
$\{W_i\}$	= global structural displacement nodal vector
$W_{\text{mech}}(\boldsymbol{w})$	= work done by mechanical forces on the structure
w_n	= structural normal displacement
w_n^{ref}	= reference structural normal displacement
$\boldsymbol{w}$	= structural displacement with normal component w_n
x_M, x_Q	= x coordinate of point M and Q
x_{M_V}, y_{M_V}, z_{M_V}	= coordinates of point M_V
$[Z_{\text{coup}}]$	= coupling impedance matrix
$[Z_{\text{ray}}]$	= radiation impedance matrix
η_s	= plate structural damping
$\Theta(\Omega)$	= frequency coherence function
ν	= plate Poisson's ratio
Π_{ac}	= radiated acoustic power
ρ_s	= plate density
ρ_0	= fluid density
Ω	= circular frequency
$\dot{(\cdot)}$	= time derivative of $(\cdot)$
$\ddot{(\cdot)}$	= second time derivative of $(\cdot)$
$\hat{(\cdot)}$	= Fourier transform of $(\cdot)$
$(\cdot)^T$	= transpose of $(\cdot)$
$(\cdot)^*$	= complex conjugate of $(\cdot)$

Received Aug. 21, 1993; revision received July 15, 1994; accepted for publication July 18, 1994.

*Ph.D. Student, G.A.U.S., Department of Mechanical Engineering, Laboratoire des Sciences de l'Habitat, E.N.T.P.E., France INSA de Lyon, France.

†Professor, G.A.U.S., Department of Mechanical Engineering. Member AIAA.

‡Professor, G.A.U.S., Department of Mechanical Engineering.

I. Introduction

SEVERAL problems of sound generation involve a mean flow past a vibrating body (e.g., aircrafts, underwater vehicles, trains). This flow may considerably affect the vibrations and the sound radiated by the structure as underlined by Crighton.[1] To improve noise prediction in such situations, it is necessary to develop methods to measure and quantify the effects of a mean flow on vibration and sound radiation patterns.

The effects of mean flow on structural stability have been largely investigated through the study of panel flutter (self-excited vibrations) (see Crighton[1] for a detailed list of references). However, not much attention has been given to the vibrational as well as the

acoustical forced response of a structure in a mean flow, when the structural displacement is not known in advance.

Several authors investigated the effect of mean flow on vibrating structures using techniques such as approximate analytical methods, modal expansion, wave number and Laplace transforms, and finite and boundary element methods: Dowling[2] and Taylor,[3] Dowell,[4–6] Dzygadlo,[7,8] Chang and Leehey,[9] Abrahams,[10] Brazier-Smith and Scott,[11] Astley,[12,13] Astley and Bain,[14] and Atalla and Nicolas.[15]

Dowling[2] analyzed the effect of mean flow on the sound generated by simple compact sources in motion (pulsating and juddering sphere) at low Mach numbers. Her analysis revealed unexpected convected features such as sound amplification in the direction normal to the source motion. Taylor[3] extended Dowling's work to noncompact vibrating bodies and confirmed Dowling's results. Dowell[4–6] studied both the flutter and the forced response due to a turbulent boundary-layer pressure fluctuation of a simply supported baffled panel immersed in a mean flow and backed by a closed rectangular cavity. In his analysis, he included nonlinear terms in the panel equation of motion and allowed for mutual interaction between the structure, the fluid inside the cavity, and the external air flow. Expanding the panel displacement in terms of its in-vacuo modes, he solved the problem using a numerical integration scheme in the time domain (mixed wave number transform and Laplace transform). As results, Dowell[4] presented several time histories of the panel velocity as well as the transmitted acoustic pressure spectrum inside the cavity. Using two different techniques, one based on a series of eigenfunctions of the in-vacuum plate for the structural displacement, the other based on a Laplace transform technique for the structural equation of the plate, Dzygadlo[7,8] obtained a solution for the problem of forced vibrations of a plate of finite length and infinite width, flown past on one side by a planar supersonic flow. His analysis allowed for mutual interaction between plate and flow and revealed a critical Mach number M_{cr} at which the system exhibits a resonance with unbounded amplitude when excited by a frequency equal to the frequency of self-excited vibrations of the plate. Below M_{cr}, the resonances of the system are bounded. Chang and Leehey[9] studied the radiation impedance and cross-modal coupling impedance of a simply supported rectangular panel in an infinite baffle in the presence of a uniform subsonic airflow, using a modal expansion in normal modes of the transverse structural displacement and a wave number transform. Their main conclusion was that mean flow increased modal radiation resistances but affected modal radiation reactance more strongly than radiation resistance. Abrahams[10] discussed the case of a compressible uniform flow past semi-infinite and finite plates using the Wiener-Hopf technique. Brazier-Smith and Scott[11] considered the case of a line-driven infinite plate in an incompressible flow. Astley[12] developed a mixed finite element method (FEM) wave envelope scheme to account for the nonuniformity of subsonic mean flow in the vicinity of the vibrating structure (vibrating cylinders and juddering spheres). In another article,[13] he developed a mixed finite element/infinite element method to include the distortion of the flow due to the plate perturbation. Astley and Bain[14] addressed the calculation of the acoustical velocity potential of a structure whose displacement is prescribed (noncoupled problem), which radiates at high frequencies in a uniform flow at low Mach number, using a modified boundary element method. Their results agreed well with analytic or other existing numerical solutions. Finally, Atalla and Nicolas[15] presented a formulation for mean flow effects on the vibro-acoustic behavior of baffled plates and studied the radiation of pistonlike radiators in the presence of mean flow. Their approach is based on a variational formulation for the plate vibrations combined with an extended Kirchhoff's integral equation to account for fluid loading. They have solved the problem using a Rayleigh-Ritz method where they have used a multipole expansion of the mean flow modified Green's function in terms of a nondimensional wave number k_0a to evaluate the radiation impedance. However, their numerical results have been limited to the piston case due to computational difficulties in evaluating higher modes (numerical instabilities in their integration scheme). They have obtained trends regarding radiation resistance and reactance in presence of mean flow, similar to those found by Chang and Leehey.

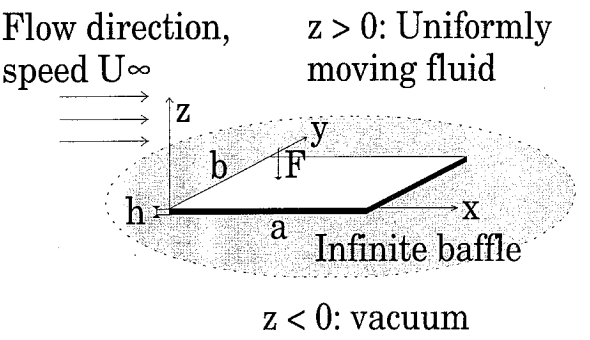

Fig. 1 Geometry of the problem—coordinate system.

This paper builds on Atalla and Nicolas's work and goes beyond their numerical difficulties. It proposes a coupled finite element/variational boundary element method that allows for the calculation of the low-frequency forced response of a point force excited baffled plate, in a uniform subsonic and inviscid mean flow. The main contribution of this paper lies in the general character of the formulation. Indeed, the analysis is based on a finite element method for the calculation of the structure transverse vibrations and the use of the extended Kirchhoff's integral equation to account for fluid loading with mean flow. A variational boundary element method (BEM) is developed to compute the acoustic radiation impedance. This general formulation can therefore be used to investigate the structural and acoustical responses of any kind of planar structures (complex shaped plates, multilayers, thick plates, etc.). A second contribution rests on the fact that the formulation shows explicitly the effects of mean flow in terms of added mass, stiffness, and radiation damping and hence allows for an insight into the physical effects of mean flow (however, structural instabilities will not be discussed). Finally, another important contribution lies in the numerical implementation of the formulation. In particular, an efficient algorithm for evaluating the different integral terms of the formulation with efficient treatment of the singularities is developed. The authors argue that the presented algorithm provides a better accuracy and avoids the difficult problem of inversion faced in the complex plane for the wave number transform approach that is commonly used as previously mentioned.

The forced response of the plate in a mean flow is investigated in both air and water. The natural frequencies of the loaded plate are shown to decrease as the Mach number increases. This effect has been found to be important in water but less pronounced in air. Furthermore, the radiated acoustic power has been found to increase sensitively with the flow speed. In air, the dominant effect amounts to a damping due to the mean flow. For water, the flow damping is negligible, and the main flow effect is a decrease of the natural frequencies with the Mach number altogether with an important increase of the radiated acoustic power. An explanation of the aforementioned changes in the acoustic power is proposed in terms of the change of the modal cross coupling and of the global radiation efficiency, induced by the flow.

This paper is organized as follows. Section II outlines the theoretical development of the analysis, and Sec. III presents the numerical implementation. In Sec. IV, the mean square velocity of the plate and the radiated acoustic power are evaluated for both the uncoupled and coupled fluid-structure problems in presence of mean flow in air and water. Finally, Sec. V offers conclusions concerning the effects of the mean flow on the forced response of the plate.

II. Theoretical Development

A. Statement of the Problem and Main Assumption

The geometry of the problem is described in Fig. 1. A rectangular flat plate embedded in an infinite rigid baffle is immersed on one side in a steady compressible potential fluid flowing along its x direction with uniform subsonic flow speed U_∞ and corresponding Mach number M_∞. The other side of the plate is in vacuum. The geometrical characteristics of the plate are indicated in Fig. 1. The fluid medium above the plate is unbounded with density ρ_0 and sound speed c_0. The plate is excited by a point force that makes it radiate sound in the moving fluid. We are interested in evaluating

the mean square velocity of the plate as well as the acoustic power radiated in the flow accounting for fluid coupling.

While vibrating, the plate creates an acoustic disturbance that propagates in the flow. Even if the plate vibrations and the acoustic field are considered to be coupled, it is assumed that mean flow remains undisturbed.

B. Equations of the Coupled System

The starting point of the formulation is Hamilton's principle for the structure. It can be written as

$$\delta \int_{t_0}^{t_1} F(w, p_{ac})\, dt = 0 \tag{1}$$

for all kinetically admissible plate displacement w satisfying $\delta w(t_0) = \delta w(t_1) = 0$.

The energy functional $F(w, p_{ac})$ associated with a plate in bending motion excited by a mechanical force and submitted to acoustical loading, in terms of the plate displacement w and the pressure p_{ac} at the surface of the plate, is given by (Bathe[16])

$$F(w, p_{ac}) = -T(w, w) + V(w, w) - W_{mech}(w) - W_{ac}(w_n, p_{ac}) \tag{2}$$

where

$$W_{mech}(w) = \int_{S_p} f(M, t) \cdot w(M, t)\, dS_M$$

and

$$W_{ac}(w_n, p_{ac}) = -\int_{S_p} p_{ac}(M, t) \cdot w_n(M, t)\, dS_M$$

The discretization of the surface S_p into finite elements and the interpolation of the structural displacement over each element allows Eq. (2) to be rewritten in terms of the nodal unknowns $\{W_i\}$ as

$$F(W_i, p_{ac}) = -\tfrac{1}{2}\{\dot{W}_i\}^T[M_s]\{\dot{W}_i\} + \tfrac{1}{2}\{W_i\}^T[K_s]\{W_i\} - \{W_i\}^T\{F_{mech}\} - \{W_i\}^T\{F_{ac}\} \tag{3}$$

where

$$\{F_{ac}\} = -[S]^T \int_{S_p} \{N^{w_n}(M)\} p_{ac}(M, t)\, dS_M \tag{4}$$

Using Eq. (3) into Eq. (1), the stationarity condition of the discretized Hamiltonian with respect to $\{W_i\}$ leads to the system

$$[M_s]\{\ddot{W}_i\} + [K_s]\{W_i\} - \{F_{mech}\} - \{F_{ac}\} = \{0\} \tag{5}$$

The expression for the mass, stiffness matrices, and the mechanical loading term can be found in classical FEM books (see, for instance, Bathe[16]). The Fourier transform of Eq. (5) leads to

$$\left(-\Omega^2[M_s] + [\tilde{K}_s]\right)\{\hat{W}_i\} = \{\hat{F}_{mech}\} + \{\hat{F}_{ac}\} \tag{6}$$

where $\hat{(\cdot)}$ denotes the Fourier transform of the quantity $[\hat{g}(\Omega) = \int_{-\infty}^{+\infty} g(t)e^{-j\Omega t}\, dt]$.

To calculate the acoustic fluid loading, the acoustic pressure on the plate should be related to the plate normal displacement. According to Atalla and Nicolas,[15] the surface pressure at a point $M(x_M, y_M, z_M = 0)$ on the plate is given by

$$\hat{p}_{ac}(M, \Omega) = -\rho_0\Omega^2 \int_{S_p} G(M, Q)\hat{w}_n(Q, \Omega)\, dS_Q + j\Omega\rho_0 c_0 M_\infty \int_{S_p} G(M, Q)\frac{\partial \hat{w}_n(Q, \Omega)}{\partial x_Q}\, dS_Q + j\Omega\rho_0 c_0 M_\infty \int_{S_p} \frac{\partial G(M, Q)}{\partial x_M}\hat{w}_n(Q, \Omega)\, dS_Q + \rho_0 c_0^2 M_\infty^2 \int_{S_p} \frac{\partial G(M, Q)}{\partial x_M}\frac{\partial \hat{w}_n(Q, \Omega)}{\partial x_Q}\, dS_Q \tag{7}$$

where

$$G(M, Q) = \frac{e^{-jk_0\tilde{R}}}{2\pi\sqrt{1 - M_\infty^2}\overset{*}{R}}$$

$$\overset{*}{R} = \sqrt{\frac{(x_M - x_Q)^2}{1 - M_\infty^2} + (y_M - y_Q)^2}$$

$$\tilde{R} = \frac{(x_Q - x_M)}{1 - M_\infty^2}M_\infty + \frac{\overset{*}{R}}{\sqrt{1 - M_\infty^2}}$$

The term $G(M, Q)$ denotes the solution of the inhomogeneous convected Helmoltz equation, subjected to the radiation Sommerfeld condition. The first term of Eq. (7) is similar to the classic Rayleigh's integral, whereas the three other terms involving $G(M, Q)$ and its derivative along the flow direction are due to the flow.

Expressing the normal displacement of the plate $\hat{w}_n$ in Eq. (7) in terms of the plate displacement nodal vector $\{\hat{W}_i\}$, one finds

$$\hat{p}_{ac}(M, \Omega) = \{C(M, \Omega)\}^T[S]\{\hat{W}_i\} \tag{8}$$

where

$$\langle C(M, \Omega)\rangle = -\rho_0\Omega^2 \int_{S_p} G(M, Q)\{N^{w_n}(Q)\}^T dS_Q + j\Omega\rho_0 c_0 M_\infty \int_{S_p} G(M, Q)\frac{\partial}{\partial x_Q}\{N^{w_n}(Q)\}^T dS_Q + j\Omega\rho_0 c_0 M_\infty \int_{S_p} \frac{\partial G(M, Q)}{\partial x_M}\{N^{w_n}(Q)\}^T dS_Q + \rho_0 c_0^2 M_\infty^2 \int_{S_p} \frac{\partial G(M, Q)}{\partial x_M}\frac{\partial}{\partial x_Q}\{N^{w_n}(Q)\}^T dS_Q \tag{9}$$

Substituting Eq. (8) into Eq. (6), one can write the coupled forced problem as

$$\left(-\Omega^2[M_s] + j\Omega[Z_{coup}] + [K_s]\right)\{\hat{W}_i\} = \{\hat{F}_{mech}\} \tag{10}$$

where $[Z_{coup}]$ is given by

$$[Z_{coup}] = [S]^T[B_{coup}][S] \tag{11}$$

where

$$[B_{coup}] = \Bigg[j\Omega\rho_0 \int_{S_p}\int_{S_p} \{N^{w_n}(M)\}G(M, Q) \times \{N^{w_n}(Q)\}^T dS_M\, dS_Q + \rho_0 c_0 M_\infty \int_{S_p}\int_{S_p} \{N^{w_n}(M)\} \times G(M, Q)\frac{\partial}{\partial x_Q}\{N^{w_n}(Q)\}^T dS_M\, dS_Q + \rho_0 c_0 M_\infty \int_{S_p}\int_{S_p} \{N^{w_n}(M)\}\frac{\partial}{\partial x_M}G(M, Q) \times \{N^{w_n}(Q)\}^T dS_M\, dS_Q - j\frac{\rho_0 c_0^2 M_\infty^2}{\Omega} \int_{S_p}\int_{S_p} \{N^{w_n}(M)\} \times \frac{\partial}{\partial x_M}G(M, Q)\frac{\partial}{\partial x_Q}\{N^{w_n}(Q)\}^T dS_M\, dS_Q \Bigg] \tag{12}$$

It is worth noting that the double surface integrals enable the removal of the singularities associated with $G(M, Q)$ and its derivative along x.

Note that for the no-flow problem, $[Z_{coup}]$ represents the classical impedance matrix for fluid structure coupled problems. Its imaginary part represents added mass and its real part the radiation damping. In case of flow, an interpretation of $[Z_{coup}]$ can only be given at lower frequencies. In this case, the first term on the right-hand side of Eq. (12) contributes mainly to the added mass; the second and third term contribute to the added damping and are proportional to $\rho_0 U_\infty$. Finally, the last term contributes principally to the added stiffness and is proportional to $\rho_0 U_\infty^2$. Note that this formulation is general and can deal with any planar structural shape.

C. Calculation of the Vibro-Acoustic Quantities

Once system (10) has been solved in terms of the plate nodal displacements $\{\hat{W}_i\}$, the mean square velocity of the plate, the acoustic pressure at a point M_v in space, and the acoustic power Π_{ac} can be recovered as shown as follows.

1. Mean Square Velocity of the Plate

The mean square velocity is calculated from the following formula:

$$\langle V^2 \rangle = \frac{\Omega^2}{2S_p} \int_{S_p} |\hat{w}_n(M, \Omega)|^2 \, dS_M$$

$$= \frac{\Omega^2}{2S_p} \{\hat{W}_i^*\}^T [S]^T \left[\int_{S_p} \{N^{w_n}(M)\} \{N^{w_n}(M)\}^T dS_M \right] [S] \{\hat{W}_i\} \tag{13}$$

2. Acoustic Pressure

The expression for the acoustic pressure at a point M_v in space is found using Eq. (8) with

$$\overset{*}{R} = \sqrt{\frac{(x_{M_v} - x_Q)^2}{1 - M_\infty^2} + (y_{M_v} - y_Q)^2 + (z_{M_v} - z_Q)^2}$$

in the expression for the modified Green's function:

$$\hat{p}_{ac}(M_v, \Omega) = \{C(M_v, \Omega)\}^T [S] \{\hat{W}_i\} \tag{14}$$

3. Radiated Acoustic Power

The acoustic power radiated in a moving flow is given by Myers[17] and can be written as

$$\Pi_{ac} = \mathrm{Re}\left[-j\frac{\Omega}{2} \int_{S_p} [\hat{p}_{ac}(M, \Omega) + \rho_0 U_\infty \hat{u}_x(M, \Omega)] \hat{u}_z^*(M, \Omega) \, dS_M \right]$$

$$= \frac{\Omega^2}{2} \mathrm{Re}[\{\hat{W}_i^*\}^T [Z_{ray}] \{\hat{W}_i\}] \tag{15}$$

where

$$[Z_{ray}] = [S]^T [B_{ray}] [S] \tag{16}$$

and

$$[B_{ray}] = \left[j\Omega\rho_0 \int_{S_p} \int_{S_p} \{N^{w_n}(M)\} G(M, Q) \{N^{w_n}(Q)\}^T dS_M \, dS_Q \right.$$

$$+ \rho_0 c_0 M_\infty \int_{S_p} \int_{S_p} \{N^{w_n}(M)\} G(M, Q) \frac{\partial}{\partial x_Q} \{N^{w_n}(Q)\}^T dS_M \, dS_Q$$

$$- \rho_0 c_0 M_\infty \int_{S_p} \int_{S_p} \frac{\partial}{\partial x_M} \{N^{w_n}(M)\} G(M, Q) \{N^{w_n}(Q)\}^T dS_M \, dS_Q$$

$$+ j\frac{\rho_0 c_0^2 M_\infty^2}{\Omega} \int_{S_p} \int_{S_p} \frac{\partial}{\partial x_M} \{N^{w_n}(M)\} G(M, Q)$$

$$\left. \times \frac{\partial}{\partial x_Q} \{N^{w_n}(Q)\}^T dS_M \, dS_Q \right] \tag{17}$$

III. Numerical Implementation

A. Calculation of the Structural Mass and Stiffness Matrices

The mass and stiffness matrices as well as the mechanical force vector of the plate have been calculated using a finite element method, based on the library of the finite element code MODULEF.[18] To model efficiently thin-plate bending, the triangular element discrete Kirchhoff's triangular plate (DKTP) element[19] was chosen to calculate the mass and stiffness matrices of the plate.

B. Numerical Evaluation of the Radiation Impedance and Treatment of Singularities

To calculate the impedance matrices (11) and (16), the surface of the plate is meshed using linear triangular elements T_i (the shape functions $\{N^{w_n}\}$ are linear). The double surface integrals in Eqs. (12) and (17) are then written as a sum of elementary integrals over triangles $T_i \times T_j$. The calculation of the integrals is simplified by mapping each surface triangular element T_i into the corresponding parent element in the reference space.

To evaluate an elementary integral involving two different triangles T_i and T_j, a Radau Hammer[20] (RH) numerical integration scheme is used. Basically, this scheme replaces the integral by a weighted sum of the integrand evaluated at a certain number of points N. The number of integration points N to be taken depends on the ratio d/λ and R/λ where d is the characteristic length of an element, R is the distance between two elements, and λ is the acoustic wavelength.

For a double surface integral involving the same element T_j, the kernels $G(M, Q)$ and $\partial G(M, Q)/\partial x_M$ become singular. To remove the singularity, the kernels are expanded into a regular part and a singular part. The regular part is evaluated using a double surface RH scheme. The singular part is first analytically integrated with respect to the first triangle in polar coordinates to remove the singularity, then numerically integrated with respect to the second triangle using an RH scheme. This semi-analytical integration removes the singularity and provides a better accuracy for the calculation of the singular integrals. It implies, though, a large amount of analytical manipulations[20] that will not be completely detailed here for the sake of conciseness. However, the key steps of the method of calculation are explained in the Appendix.

IV. Results for the Forced Response of a Plate in a Mean Flow

The proposed formulation has been validated and was shown to provide good results for fluids at rest and for pistonlike radiators in a uniform mean flow.

To study the effects of mean flow on the vibro-acoustic behavior of the plate (i.e., its mean square velocity and radiated acoustic power), two situations will be considered: light fluid (air) and heavy fluid (water). The numerical experiments shown here considered an aluminum plate with structural damping $\eta_s = 0.01$ excited by a point force of amplitude $0.5N$, located on the plate at ($x = 0.3275$, $y = 0.2875$). The characteristics of the plate were $a = 0.455$ m, $b = 0.375$ m, $E = 7.2 \times 10^{10}$ Pa, $h = 2.5$ mm, $\nu = 0.3$, and $\rho_s = 2700$ kg/m^3. The values of density and sound speed were $\rho_0 = 1$ kg/m^3 and $c_0 = 340$ m/s in air and $\rho_0 = 1000$ kg/m^3 and $c_0 = 1460$ m/s in water. A regular mesh of 16×13 nodes was used for the calculations.

A. In Air

Results are presented in Figs. 2–4. Both the noncoupled (Fig. 2) and the coupled problems (Figs. 3 and 4) were investigated. Figure 2 shows the effect of mean flow on the radiated sound power when fluid loading is neglected (i.e., noncoupled problem). This is done by first solving for the vibrations of the plate, neglecting fluid loading and mean flow effects, then calculating the radiated acoustic power in the presence of mean flow. As can be seen in Fig. 2, the effect of flow is negligible for small Mach numbers ($M_\infty < 0.2$). For higher Mach numbers, there is an increase of the radiated acoustic power brought in by the mean flow. Figures 3 and 4 show the same trends, but this time fluid loading and mean flow effects are accounted for in the vibrational response of the plate. Figure 3 shows the effect on the mean square velocity and Fig. 4 on the radiated acoustic

Table 1 First three resonance peaks (in Hz) in air at $M_\infty = 0$ and 0.6; case i: first + fourth term of Eq. (12), case ii: all terms of Eq. (12)

Mach number,	Mode 1 (1, 1)		Mode 2 (2, 1)		Mode 3 (1, 2)	
M_∞	Case i	Case ii	Case i	Case ii	Case i	Case ii
0	——	72.2	——	160.5	——	202.3
0.6	67.0	66.5	153.6	152.7	201.1	200.9

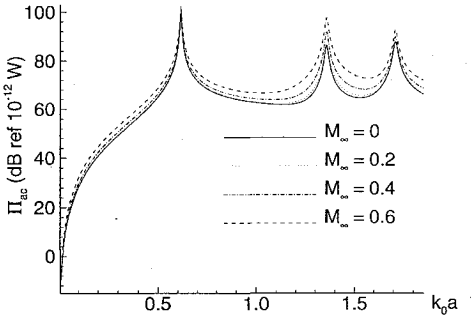

Fig. 2 Acoustic power in the case of the noncoupled problem in air for M_∞ = 0, 0.2, 0.4, and 0.6.

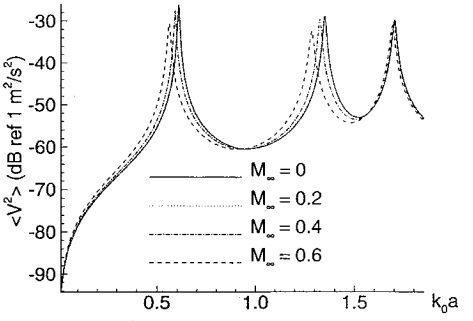

Fig. 3 Mean square plate velocity in the case of the coupled problem in air for M_∞ = 0, 0.2, 0.4, and 0.6.

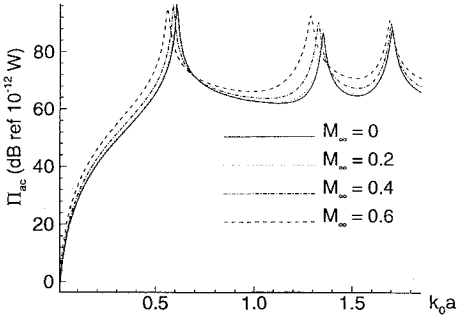

Fig. 4 Acoustic power in the case of the coupled problem in air for M_∞ = 0, 0.2, 0.4, and 0.6.

power. Once again, mean flow effects are negligible for small Mach numbers but are important for higher Mach numbers.

The major effect appearing in both the noncoupled and coupled cases is a global increase of the radiated acoustic power with the flow speed. An explanation of this phenomenon may be found in the increase of the global radiation efficiency of the plate with the Mach number. Indeed, this increase is clearly exhibited when calculating the radiation efficiencies of the plate, in the case of the coupled problem for air at rest and for air moving at a Mach number equal to 0.6. In addition, at low frequencies, the modal radiation efficiencies were found to increase with the flow speed (results not reported here for conciseness). Note that similar conclusions are obtained in the case of the noncoupled problem. In the latter case, mean flow makes all of the structural modes more efficient acoustic radiators. This is easily understandable in the case of the noncoupled problem, since the additional energy brought in by the flow does not modify the vibratory energy and cannot be transferred from one mode to another through modal coupling. Therefore, the structure dissipates more energy in the form of acoustic energy at all frequencies. In the case of the coupled problem, this is more complex since the supplementary energy convected by the flow may be redistributed into acoustic as well as vibratory energy. Indeed, through fluid coupling, vibratory energy can be mutually transferred between radiating and nonradiating structural modes. As discussed in the next section, a way of explaining the increase of radiation efficiency and the decrease of the mean square velocity of the plate may be found in the cross-modal coupling induced by the mean flow.

The coupled problem (Figs. 3 and 4) shows fundamental differences with the noncoupled situation. First, there is a decrease of the natural frequencies of the plate due to mean flow. This is apparent in Figs. 3 and 4 through the leftward shift of the resonance peaks of both the mean square velocity and the radiated power. This shift increases with Mach numbers, but it is negligible for Mach numbers less than 0.2. The observed shift in the natural frequencies actually results from the importance of fluid coupling due to mean flow. In the no-flow case, fluid loading effects are twofold, added mass and acoustic radiation damping, both being negligible in air. In case of mean flow, as discussed in the formulation (at least at lower frequencies), flow coupling effects comprise added mass, added stiffness, and acoustic radiation damping. Since the added mass term is independent of the flow speed and has been checked to be negligible for air, it is reasonable to think that the shift effect is mainly due to the added stiffness. To show this, the coupled problem is solved when the damping effects are neglected [i.e., neglecting the second and third terms accounting for damping in the expression of $[Z_{coup}]$ in Eq. (11)]. Table 1 summarizes the results for $M_\infty = 0.6$. It compares the position of the resonance peaks for the first three modes of the plate, with and without the flow added damping terms. The positions of the resonance peaks at $M_\infty = 0$ are also given to show the extent of the frequency shift induced by the flow. From Table 1, it is clearly seen that in air the added stiffness is in a large part responsible for the resonance frequencies shift. This shift being leftward, the added stiffness effect is negative.

Second, added damping effects due to mean flow show up clearly in Fig. 3 where the classical damping trends are found (widening of the resonance peaks and decrease of the peaks amplitude). This damping effect increases with the flow speed, which is consistent with Eq. (12) (i.e., the damping term is proportional to $\rho_0 U_\infty$). Indeed, Table 1 shows that the shift of frequency brought in by the damping term is small.

The previous discussion indicates that the different effects of mean flow, that is to say, the decrease of the resonance frequencies, the added damping and increase of the radiated acoustic power, cannot be neglected for higher Mach numbers even for a light fluid.

Finally, it should be noted that one must be aware that, above a critical value of U_∞, structural instabilities start occurring (e.g., divergence and flutter instabilities), making this linear theory not adapted. The study of these instabilities is, however, not the purpose of this paper.

B. In Water

The purpose of this section is to discuss the effect of mean flow for a heavy fluid with a small Mach number. The coupled problem in water, without and with mean flow, was considered. In the latter,

Table 2 First three resonance peaks (in Hz) in water at $M_\infty = 0$ and 0.007; case i: first + fourth term of Eq. (12), case ii: all terms of Eq. (12)

Mach number,	Mode 1 (1, 1)		Mode 2 (2, 1)		Mode 3 (1, 2)	
M_∞	Case i	Case ii	Case i	Case ii	Case i	Case ii
0	—	14.4	—	46.0	—	61.2
0.007	12.2	11.6	42.2	42.6	60.5	59.2

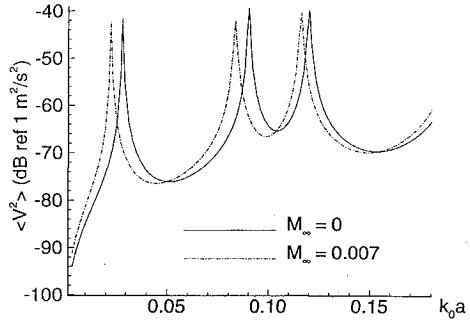

Fig. 5 Mean square plate velocity in the case of the coupled problem in water for M_∞ = 0 and 0.007.

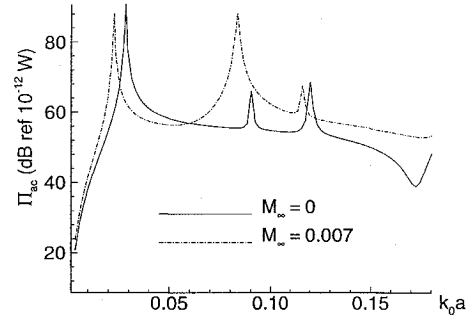

Fig. 6 Acoustic power in the case of the coupled problem in water for M_∞ = 0 and 0.007.

a Mach number equal to 0.007 (U_∞ = 10.2 m/s) was used. Figures 5 and 6 show, respectively, the obtained mean square velocity and radiated acoustic power. Since there is a strong modal density in the frequency range studied here, only the first three modes are considered for the sake of clarity.

As seen in Figs. 5 and 6, the effect of the flow appears to be more important on the radiated acoustic power than on the mean square velocity of the plate. As in the case of air, there is a decrease of the resonance frequencies of the plate. This decrease is important at low frequencies but seems to weaken at higher frequencies. However, in contrast with the results in air, the shift is important even at small Mach numbers. As in air, the negative added stiffness has been found to be mainly responsible for this effect. Table 2 compares the position of the resonance peaks for the first three modes of the plate in water, with and without the flow added damping terms. It appears that, for the first two modes [i.e., Mode (1, 1) and (2, 1)], the negative added stiffness term is, in a large part, responsible for the natural frequencies shift. However, as the frequency increases, the contributions of the damping and stiffness terms become of equal importance.

Figure 5 shows that the damping effect is less pronounced than in air. This is logical since it can be seen from Eq. (12) that the ratio of the added damping term to the inertia term is proportional to $U_\infty/(\Omega a)$. For the range of frequencies and flow speeds considered (i.e., U_∞ = 10 m/s in water), this ratio is much smaller in the case of water compared with air.

As in air, the radiated acoustic power globally increases with the flow speed except for modes (1, 1) and (1, 2). In particular, the increase of the radiated power appears to be particularly pronounced for mode (2, 1) (cf. Fig. 6). This is partially corroborated by the

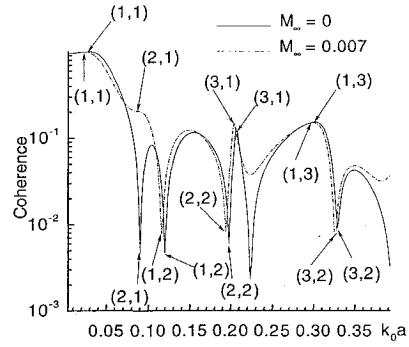

Fig. 7 Coherence function for mode (1, 1) in water for M_∞ = 0 and 0.007.

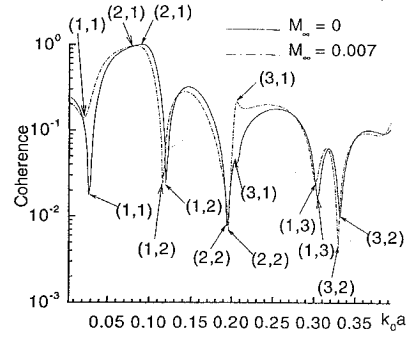

Fig. 8 Coherence function for mode (2, 1) in water for M_∞ = 0 and 0.007.

calculation of the radiation efficiency of the plate that decreases with the flow speed for mode (1, 1) and (1, 2) but increases for modes (2, 1). Another possible explanation for these changes in the radiated acoustic power may be found in the extra modal coupling brought in by the mean flow. To quantify this modal coupling, a frequency coherence function (see Figs. 7 and 8) between a reference modal shape and the structural shape of the plate $\hat{w}_n$ at frequency Ω is defined as follows:

$$\Theta(\Omega) = \frac{\left|\int_S \hat{w}_n(M,\Omega)\cdot \hat{w}_n^{\text{ref}*}(M,\Omega)\mathrm{d}S_M\right|}{\sqrt{\int_S |\hat{w}_n(M,\Omega)|^2\,\mathrm{d}S_M}\sqrt{\int_S |\hat{w}_n^{\text{ref}}(M,\Omega)|^2\,\mathrm{d}S_M}} \tag{18}$$

This function indicates, at each frequency, the correlation between the normal displacement field of the plate and the reference modal shape. The reference modal shapes were chosen as the in-vacuum modal shapes of a simply supported baffled plate. The in-vacuum modal shapes have been chosen for their accuracy and the simplicity of their numerical implementation. Figures 7 to 8 show coherence functions for two reference modal shapes corresponding to the first two in-vacuum modes [modes (1, 1) and (2, 1)] for M_∞ = 0 and 0.007. In the no-flow case, the classical conclusions (Berry[21,22]) concerning the importance of coupling between odd-odd modes in a heavy fluid, are seen in these figures. For instance, Fig. 7 shows that for the (1, 1) mode the coupling is more important with the (1, 3) and (3, 1) modes than with the other modes (i.e., odd-even, even-odd, and even-even modes). However, in the case of flow it is seen that the flow introduces a strong coupling even between modes that were weakly coupled in the no-flow case. Note, for example,

the importance of coupling between the (1, 1) and (2, 1) modes in Fig. 7. Since this coupling phenomenon expresses energy transfer between different modes, modes that radiate weakly in the no-flow case may become important radiators in presence of mean flow and the converse. This may explain the global increase of radiated acoustic power in the presence of mean flow. Figure 8 confirms these trends. These explanations have also been checked for the case of air using the previous coherence function. In conclusion, keeping in mind the simplicity of the criterion defined by Eq. (18), the modal cross coupling brought in by the mean flow may be responsible for the global increases in the acoustic power radiated by the plate.

V. Conclusion

In this paper, an FEM-BEM implementation of a general formulation for the vibro-acoustic analysis of a flat plate past which there is a uniform mean flow has been presented. This formulation shows explicitly the effects of the mean flow in terms of added mass, damping, and stiffness. Excellent agreement has been obtained between this approach and the existing literature in the no-flow case and for pistonlike radiators in mean flow.

A discussion of the effect of mean flow on the vibro-acoustic indicators of the plate has been presented. In particular, two situations have been considered: light fluid (air) but large mean flow and heavy fluid (water) but small mean flow.

In air, the effect of fluid loading may be neglected for small Mach numbers ($M_\infty < 0.2$). But at higher Mach numbers fluid coupling is no longer negligible. One of its effects is to decrease the natural frequencies of the plate. It has been found that this is mainly due to the negative stiffness added by the mean flow, which may also lead to structural instabilities (not investigated here). Another important mean flow effect is an increase of the radiation damping that causes a damping of the vibrations of the plate and a global increase of the radiated acoustic power.

In water, the previous conclusions hold even for small flow speeds. An investigation of cross-modal coupling introduced by the flow has been discussed. It has indicated that in both air (with large Mach numbers) and water (even at small Mach numbers) cross-modal coupling becomes important. This coupling may also explain, to some extent, the global increase of the radiated power in the presence of mean flow.

Appendix: Method of Calculation of the Singular Parts

The calculation of $[Z_{\text{coup}}]$ and $[Z_{\text{ray}}]$ requires the computation of matrix terms of the form

$$[A_1] = \int_{S_p}\int_{S_p} \{N^{w_n}(M)\}K(M, Q)\{N^{w_n}(Q)\}^T \mathrm{d}S_M\, \mathrm{d}S_Q \quad \text{(A1)}$$

and

$$[A_2] = \int_{S_p}\int_{S_p} \{N^{w_n}(M)\}K(M, Q)\frac{\partial}{\partial x_Q}\{N^{w_n}(Q)\}^T \mathrm{d}S_M\, \mathrm{d}S_Q \quad \text{(A2)}$$

where $K(M, Q)$ denotes the modified Green function or its derivative. When the surface S is discretized into linear triangles (linear shape functions) T_i, $[A_1]$ and $[A_2]$ can be rewritten in terms of the area coordinates over each reference triangles, namely, (ξ_1, ξ_2, ξ_3) over t_i and (η_1, η_2, η_3) over t_j (Fig. A1). Then,

$$[A_1] = 4\Sigma_i\Sigma_j S_i S_j \int_{t_i}\int_{t_j} \xi_k\eta_l K(M, Q)\,\mathrm{d}t_i\,\mathrm{d}t_j, \quad (k, l) \in [1, 3]^2 \quad \text{(A3)}$$

$$[A_2] = 2\Sigma_i\Sigma_j S_i R^j_{1e} \int_{t_i}\int_{t_j} \xi_k K(M, Q)\,\mathrm{d}t_i\,\mathrm{d}t_j, \quad (k, l) \in [1, 3]^2 \quad \text{(A4)}$$

where the sign Σ is to be understood in the matrix assembling sense, and S_i and S_j denote the surfaces of the triangles T_i and T_j of interest and come from the Jacobian of the change of variables in terms of the normal coordinates (ξ_1, ξ_2, ξ_3). For each triangle T_j, R^j_{pl} is a transformation matrix given by

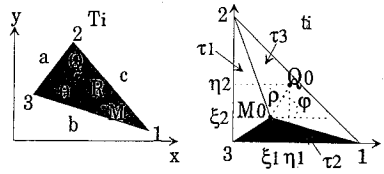

Fig. A1 Semi-analytical integration.

$$R^j_{pl} = \begin{bmatrix} y^j_2 - y^j_3 & y^j_3 - y^j_1 & y^j_1 - y^j_2 \\ x^j_1 - x^j_2 & x^j_1 - x^j_3 & x^j_2 - x^j_1 \end{bmatrix} \quad \text{(A5)}$$

where (x^j_p, y^j_p), $p \in [1, 3]$, denote the coordinates in the real space of each vertex of triangle T_j.

As noticed in Sec. III, the numerical difficulty resides in the computation of $[Z_{\text{coup}}]$ and $[Z_{\text{ray}}]$ when the triangles intervening in the double surface integral are the same. In this case, the kernels become singular and a semi-analytical integration scheme is proposed to evaluate the integrals of concern, which are of the form

$$D_{kl} = \int_{t_i}\int_{t_i} \xi_k\eta_l K(M, Q)\,\mathrm{d}t_i\mathrm{d}t_i, \qquad (k, l) \in [1, 3] \times [0, 3] \quad \text{(A6)}$$

where we have defined η_0 as 1.

To calculate D_{kl}, $K(M, Q)$ is split into a regular part that is integrated numerically with a double surface Radau Hammer (RH) integration scheme and a singular part that is semi-analytically integrated to eliminate the singularity and then seminumerically integrated with a single surface RH integration scheme. The singular parts are of the form

$$C_{mnkl} = \int_{t_i}\int_{t_i} \xi_k\eta_l \frac{(x_M - x_Q)^m}{\overset{*}{R}{}^n}\,\mathrm{d}t_i\,\mathrm{d}t_i,$$

$$(m, n, k, l) \in [0, 3] \times [1, 3] \times [1, 3] \times [0, 3] \quad \text{(A7)}$$

Figure A1 shows a triangle T_i in the real space and the corresponding triangle t_i mapped in the reference space (normal coordinates). Let M and Q be two points of triangle T_i (real space). These points are mapped onto the reference triangle t_i into M_0 and Q_0. Coordinates (ξ_1, ξ_2, ξ_3) refer to point M_0 and (η_1, η_2, η_3) to point Q_0. The distance between M and Q is denoted R, and the distance between M_0 and Q_0 is denoted ρ; θ refers to the angle at vertex 3 of the triangle of concern T_i in the real space shown in Fig. A1.

In this paper, the so-called method of semi-analytical integration consists in integrating C_{mnkl} with respect to $(\eta_1, \eta_2,)$. Let φ denote the angle between the line (M_0, Q_0) and the horizontal axis. The integration with respect to $(\eta_1, \eta_2,)$ is achieved using the change of variables:

$$\begin{cases} \eta_1 = \xi_1 + \rho\cos\varphi \\ \eta_2 = \xi_2 + \rho\sin\varphi \end{cases} \quad \text{(A8)}$$

From Fig. A1, the following relationships are derived:

$$\overset{*}{R}(\xi_1, \xi_2, \eta_1, \eta_2) = \sqrt{a^2(\xi_2 - \eta_2)^2 + b^2(\xi_1 - \eta_1)^2 + 2(\xi_1 - \eta_1)(\xi_2 - \eta_2)ab\cos\theta} \quad \text{(A9)}$$

where

$$a^2 = \frac{x^2_{23}}{1 - M^2_\infty} + y^2_{23}, \quad b^2 = \frac{x^2_{13}}{1 - M^2_\infty} + y^2_{13} \quad \text{(A10)}$$

$$x_M - x_Q = (\xi_1 - \eta_1)x_{13} + (\xi_2 - \eta_2)x_{23} \quad \text{(A11)}$$

Expressing $x_M - x_Q$ and $\overset{*}{R}$ in terms of ρ and φ yields

$$\overset{*}{R}(\rho, \varphi) = \rho\sqrt{a^2 \sin^2 \varphi + b^2 \cos^2 \varphi + 2ab \cos\theta \cos\varphi \sin\varphi}$$
$$= \rho f(\varphi) \tag{A12}$$

$$x_M - x_Q = -\rho[x_{13} \cos\varphi + x_{23} \sin\varphi] = -\rho g(\varphi) \tag{A13}$$

Using Eqs. (A8), (A12), and (A13), C_{mnkl} can then be rewritten as

$$C_{mnkl} = \int_{t_i} \xi_k \int_{t_i} \frac{\Psi_{mn}(\rho, \varphi, \xi_l)}{f^n(\varphi)} \rho \, d\rho \, d\varphi \, d\xi_1 \, d\xi_2 \tag{A14}$$

Finally, the integrals with respect to (ρ, φ) that have to be calculated amount to the calculation of terms of the form

$$I_n(\boldsymbol{\xi}) = \int_{t_i} \frac{h(\rho, \varphi, \xi_1, \xi_2)}{f^n(\varphi)} d\rho \, d\varphi = \int_{\tau_1} \frac{h(\rho, \varphi, \xi_1, \xi_2)}{f^n(\varphi)} d\rho \, d\varphi$$
$$+ \int_{\tau_2} \frac{h(\rho, \varphi, \xi_1, \xi_2)}{f^n(\varphi)} d\rho \, d\varphi + \int_{\tau_3} \frac{h(\rho, \varphi, \xi_1, \xi_2)}{f^n(\varphi)} d\rho \, d\varphi \tag{A15}$$

where $\boldsymbol{\xi}$ denotes the vector (ξ_1, ξ_2, ξ_3), and $h(\rho, \varphi, \xi_1, \xi_2)$ is a polynomial in the variables ρ, $\cos\varphi$, $\sin\varphi$, ξ_1, and ξ_2.

Integrating with respect to ρ over each subtriangles τ_1, τ_2, τ_3, $I_n(\boldsymbol{\xi})$ becomes

$$I_n(\boldsymbol{\xi}) = \int_{\varphi_2}^{\varphi_3} \frac{h_1(\varphi, \xi_1, \xi_2)}{f^n(\varphi)} d\varphi + \int_{\varphi_3}^{\varphi_1} \frac{h_2(\varphi, \xi_1, \xi_2)}{f^n(\varphi)} d\varphi$$
$$+ \int_{\varphi_1}^{\varphi_2} \frac{h_3(\varphi, \xi_1, \xi_2)}{f^n(\varphi)} d\varphi \tag{A16}$$

where

$$h_1(\varphi, \xi_1, \xi_2) = \int_0^{-\frac{\xi_1}{\cos\varphi}} h(\rho, \varphi, \xi_1, \xi_2) \, d\rho \tag{A17}$$

$$h_2(\varphi, \xi_1, \xi_2) = \int_0^{-\frac{\xi_2}{\sin\varphi}} h(\rho, \varphi, \xi_1, \xi_2) \, d\rho \tag{A18}$$

$$h_3(\varphi, \xi_1, \xi_2) = \int_0^{\frac{\xi_3}{\cos\varphi + \sin\varphi}} h(\rho, \varphi, \xi_1, \xi_2) \, d\rho \tag{A19}$$

Finally, the integration of $h1$, $h2$, and $h3$ with respect to φ is done analytically using multiple algebraic manipulations that will not be detailed here for the sake of conciseness (cf. Sgard and Atalla[20]).

Acknowledgments

The authors would like to acknowledge the financial support of the National Science and Engineering Council of Canada and the Laboratoire des Sciences de l'Habitat (E.N.T.P.E, France). The authors also wish to thank P. Myers (the George Washington University) for valuable discussions on the definition of the radiated acoustic power in presence of mean flow.

References

[1]Crighton, D. G., "The 1988 Rayleigh Medal Lecture: Fluid Loading—The Interaction Between Sound and Vibration," *Journal of Sound and Vibration,* Vol. 133, No. 1, 1989, pp. 1–27.

[2]Dowling, A., "Convective Amplification of Real Simple Sources," *Journal of Fluid Mechanics,* Vol. 74, No. 3, 1976, pp. 529–546.

[3]Taylor, K., "Acoustic Generation by Vibrating Bodies in Homentropic Potential Flow at Low Mach Number," *Journal of Sound and Vibration,* Vol. 65, No. 1, 1979, pp. 125–136.

[4]Dowell, E. H., "Noise or Flutter or Both," *Journal of Sound and Vibration,* Vol. 11, No. 2, 1970, pp. 159–180.

[5]Dowell, E. H., "Nonlinear Oscillations of a Fluttering Plate," *AIAA Journal,* Vol. 4, No. 7, 1966, pp. 1267–1275.

[6]Dowell, E. H., "Flutter of Plates and Shells. Part I: Plate," *AIAA Journal,* Vol. 4, No. 8, 1966, pp. 1370–1377.

[7]Dzygadlo, Z., "Forced Vibration of a Plate of Finite Length in Plane Supersonic Flow (I)," *Proceedings of Vibration Problems,* Vol. 1, No. 8, 1967, pp. 61–77.

[8]Dzygadlo, Z., "Forced Vibration of a Plate of Finite Length in Plane Supersonic Flow (II)," *Proceedings of Vibration Problems,* Vol. 2, No. 8, 1967, pp. 155–170.

[9]Chang, Y. M., and Leehey, P., "Acoustic Impedance of Rectangular Panels," *Journal of Sound and Vibration,* Vol. 64, No. 2, 1979, pp. 243–256.

[10]Abrahams, I. D., "Scattering of Sound by an Elastic Plate with Flow," *Journal of Sound and Vibration,* Vol. 89, No. 2, 1983, pp. 213–231.

[11]Brazier-Smith, P. R., and Scott, J. F., "Stability of Fluid Flow in the Presence of a Compliant Surface," *Wave Motion,* 6, 1984, pp. 547–560.

[12]Astley, R. J., "A Finite Element, Wave Envelope Formulation for Acoustical Radiation in Moving Flows," *Journal of Sound and Vibration,* Vol. 103, No. 4, 1985, pp. 471–485.

[13]Astley, R. J., "Wave Envelope and Infinite Element Schemes for Acoustical Radiation," *International Journal for Numerical Methods in Fluids,* Vol. 3, 1983, pp. 507–526.

[14]Astley, R. J., and Bain, J. G., "A Three-Dimensional Boundary Element Scheme for Acoustic Radiation in Low Mach Number Flows," *Journal of Sound and Vibration,* Vol. 109, No. 3, 1986, pp. 445–465.

[15]Atalla, N., and Nicolas, J., "A Formulation for Mean Flow Effects on Sound Radiation from Rectangular Baffled Plates with Arbitrary Boundary Conditions," *International Symposium on Flow-Induced Vibration Noise,* American Society of Mechanical Engineers, NCA-Vol. 13, 1992, pp. 69–84.

[16]Bathe, K. J., *Finite Element Procedures in Engineering Analysis,* Prentice-Hall, Englewood Cliffs, NJ, 1982.

[17]Myers, M. K., "Transport of Energy by Disturbances in Arbitrary Steady Flows," *Journal of Fluid Mechanics,* Vol. 226, 1991, pp. 383–400.

[18]Anon., MODULEF, INRIA, Domaine de Voluceau, Rocquencourt BP 105-78153 LE CHESNAY, France.

[19]Touzot, J. L., and Dhatt, G., *Modélisation des Structures par Éléments Finis, Poutres et Plaques,* Vol. 2, Les Presses de l'Université Laval, Québec, Canada, 1992.

[20]Sgard, F. C., and Atalla, N., "Calcul des intégrales intervenant dans l'impédance de rayonnement acoustique d'une plaque bafflée dans un écoulement uniforme," University of Sherbrooke, Int. Report, Groupe d'Acoustique de l'Université de Sherbrooke, Sherbrooke, Québec J1K 2R1, Canada, 1992.

[21]Berry, A., Guyader, J. L., and Nicolas, J., "A General Formulation for the Sound Radiation from Rectangular, Baffled Plates with Arbitrary Boundary Conditions," *Journal of the Acoustical Society of America,* Vol. 88, No. 6, 1990, pp. 2792–2802.

[22]Berry, A., "A New Formulation for the Vibration and Sound Radiation of Fluid-Loaded Plates with Elastic Boundary Conditions," *Journal of the Acoustical Society of America* (to be published).